DALTON PERSPECTIVE

Molecular precursors for (nano) materials — a one step strategy

Michael Veith

Universität des Saarlandes, Institut für Anorganische Chemie, Saarbrücken, Germany

Received 6th February 2002, Accepted 5th April 2002
First published as an Advance Article on the web 20th May 2002

The use of molecular Single Source Precursors (SSP) containing all elements necessary for the formation of the final solid material in CVD (Chemical Vapor Deposition) or sol–gel routes is classified with respect to the control of the reaction. Three different cases have been distinguished: In SSP-I the stoichiometric ratio of the elements in the precursor corresponds to the ratio required in the solid whereas the number and kind of side products of the reaction (ligands) are not controlled. In SSP-II, not only does the ratio of the elemental components of the precursor have the correct stoichiometry but also the ligands are chosen in such a way that a cascade of reactions is induced at moderate temperatures leading to few products and therefore low contamination of the solid material. In SSP-III, the precursor decomposes to form at least two solid phases with perfect stoichiometric and structural control. All three processes allow the obtention of nanocrystalline materials.

Born in 1944 in Goerlitz, Germany, Michael Veith studied chemistry at the University of Munich, receiving his Diplom-Chemiker degree in 1969. Continuing work with Prof. N. Wiberg, he obtained his doctoral degree in 1971 and then moved to the University of Karlsruhe where he started his postdoctoral work with Prof. H. Bärnighausen, completing his Habilitation in inorganic chemistry in 1977. He was Privat-Dozent at the University of Karlsruhe until the end of 1978 when he moved to the Technische Universität Braunschweig as a Professor of Inorganic Chemistry. He moved to the University of Saarland (Saarbrücken) in 1984 and became Full Professor. He has received several awards including the Heisenberg Scholarship (1978), Winnacker Scholarship (1978), Academy Prize for Chemistry of the Academy of Sciences (1982), the Lleibniz-Preis (1991) and the Victor Grignard–Georg Wittig lectureship (1994). Since 1997 he has been a member of the SFB Senat-Comitee of the DFG inBonn. His main research interests are in synthetic and structural chemistry, particularly relating to molecular compounds containing metal elements.

Michael Veith

Introduction

The impact of chemical methods in materials science seems to have increased in recent times as may be deduced from the steady increase in published reports and the appearance and extension of journals dedicated to this special subject.[1] Two processes appear to be driving forces in this evolution: the chemical vapor deposition (CVD) technique and the sol–gel process.[2–7] In the CVD method molecular precursors are transported through the gas phase and thermolyzed to liberate volatile entities and a solid residue, which can either be coated onto the surface of a substrate or gathered as a powder. Normally several precursors are used which may react together or separately, to fulfill the elemental combination of the material to be synthesized. Many different methods have been developed to activate the molecules (oven, induction fields, lasers, plasmas, flames *etc.*), which can be transported in gas streams or at reduced pressure. There are a number of abbreviations used which characterize the pecularity of the technique like MO-CVD (metal organic chemical vapor deposition) PA-CVD (plasma assisted CVD) *etc.*[2] The other important approach, the sol–gel process, uses molecules, salts or metal complexes which are mixed in a stoichiometric ratio in a solvent where they are slowly activated by traces of protonic reactants, the most common being water. As a result of this activation, polycondensation reactions occur which generally lead to a sol or a gel composed of a mixture of compounds.[5] By aging or heating, volatiles are liberated from the sol–gel mixture and the residue is transformed to a solid material. As in the case of the CVD approach the process can be used to obtain powders of the material or coatings on different substrates. To obtain films several techniques like dip coating or spin coating have been developed to deposit the intermediate sol–gel mixture onto substrates.[8,9]

While in the early stages of the development of CVD and sol–gel techniques only single phase products like III/V semiconductors (GaAs) or oxide ceramics[10,11] were targeted, more recently composites or hybrid materials have also been obtained. The sol–gel process is particularly well suited to synthesize, for example, metallic phases in ceramics[12] or to combine the silicon–oxygen backbone of silicon dioxide with an organic polymer or linker.[13,14]

Solid biphasic composites can belong to the three following categories: solid/solid, solid/liquid or solid/gas. Either the mechanical or physical properties of such composites may be of interest, *e.g.*: metal sponges (solid/gas) may be useful for techniques requiring large surface areas (catalysts), solid colloids (solid/solid) may be used for their light scattering properties (naturally occurring gems), mixtures of ceramics and metal phases (solid/solid) have quite interesting material properties which make them useful for interfaces between metal and ceramic surfaces, equally distributed metallic phases in ceramics (solid/solid) may be used as quantum dots, mixtures of ceramics and polymer fibers (solid/liquid) may have interesting elastic constants. This list is of course incomplete and can be

DOI: 10.1039/b201383p

extended *ad libitum*. It is obvious that techniques other than CVD or sol–gel may be used to obtain the desired composites. As a matter of fact, ball milling,[15] ion implantation,[16] plasma spray and electro deposition of ceramic powders[17] are the often employed techniques. They have the advantage of being easily useable but the disadvantage of limited tunability, especially when the ratio of the sizes of the different phases in the composite have to be adjusted. When the diameters of the different phases approach the nanometer scale, it is obvious that new techniques or variations have to be considered.

While bulk materials have characteristic physical properties, these may drastically change when the nano-scale is reached. Gleiter has shown that Ni powders with mean diameters of several nanometers, obtained from a gas condensation process, have different thermodynamical constants than ordinary μm powders.[18] Meanwhile this nano-technology has been extended to ceramics, alloys and other classical materials and the "size-effect" on the physical properties is now a well accepted principle.[18–20]

At this point it seems important to recall, that chemistry — especially low molecular chemistry — typically running on a scale between 0.1 to 2 nm is an ideal starting point for building up larger entities. The chemical approach to nano-sciences is therefore a bottom-up (building up) process while the standard techniques employed by engineers are the so-called top down (cutting down) techniques. The question is: how do we have to modify the well known processes like CVD and sol–gel to obtain defined nano-scaled materials?

The following article compiles some attempts undertaken in our laboratory to answer this question. It is a very personal view of the subject and the "single source precursor" strategy is not a new idea, but has been developed by different scientists with different emphasis given to its use.[21–23] I would also like to draw attention to several reviews dealing with molecular precursor approaches in general.[24–26] At this stage it should also be recalled that not every assembly of components in the precursor is reflected by the elemental ratios in the final product as the chemical bonding in the precursors plays an important role, especially in the gas phase. I will not discuss these problems here, but it is obvious that the choice of ligands and elements is a crucial step in the single source precursor strategy if undesired side reactions are to be avoided. Furthermore, I would like to highlight a couple of articles which have been published as predecessors of this perspective.[27–30]

The single source precursor concept

In a gas phase (CVD) or solution process (sol–gel) a "single source precursor" (SSP) is usually a molecular compound which contains all the necessary elements of the final product in a well defined molecule. Sometimes the same term is also used for a molecular or ionic aggregate of defined stoichiometry formed as an intermediate in a "one pot" sol–gel process.[23] We will not consider this second definition further here. The definition given so far can be subdivided into three different cases:

1. In the first case, which we will term SSP-I, not only the correct elements are assembled in the starting molecule but the elements are also present in the correct stoichiometric ratio of the final product. In eqn. (1) this is illustrated by two components A and B (A and B denote either elements or distinct formula units) and "ligands" X and Y which are liberated as such or in a modified way (X and Y may split off into further species) during the process.

$$\text{SSP-I:}\quad AB_nXY \longrightarrow AB_n + X + Y \qquad (1)$$

Of course besides A and B other components may be assembled in the precursor and the ligands X and Y or the transformed ones may also deviate from unity.

2. In the second case, SSP-II, the elemental components of the precursor (A, B *etc.*) are in the correct stoichiometry of the final product, but also the ligands of the precursor are chosen in such a way that chemical reactions are somewhat "preformed". Already at *low temperatures* cascades of reactions are started leading to only a *few perfectly defined* products and consequently the contamination of the material with undesired side products is limited. The low process temperature is especially useful for the formation of small sized particles as the growth of the phases is slowed down. In eqn. (2) one example is given, the combination of X and Y to a volatile and/or inert molecule being the key step of a simple pseudo one step cascade:

$$\text{SSP-II:}\quad AB_nXY \longrightarrow AB_n + X\text{–}Y \qquad (2)$$

Instead of one single volatile product several species may be formed depending on the number of ligands X and Y in a precursor molecule and the cascade may also consist of several steps.

3. The third case, SSP-III, represents an even more complex situation in which a *multi phase system* of at least two solid phases is obtained from a single precursor molecule in *controlled stoichiometry*. This is evidently a very interesting procedure as the two phases formed have the chance to interpenetrate on a molecular level and, as they originate from a common molecular source, their three-dimensional distribution and the grain sizes of the phases can be easily controlled by temperature, concentration of activators (sol–gel) or pressure (CVD). A general equation, (3), for such a process may be formulated, although the chemical back-ground for such reactions may be quite complex.

$$\text{SSP-III:}\quad AB_nXY \longrightarrow AB_{n-m} + mB + X\text{–}Y \qquad (3)$$

As we shall show further (*vide infra*), disproportionations of metastable oxidation states of metallic elements may lead to metal/metal oxide composites or thermodynamics may be used to create a composite of two different metal oxide phases. Also, intermediates formed in the thermal decomposition processes of precursors may re-enter the cascades of reactions leading to alloys in metal oxide matrices.

In the following sections we will illustrate the above classification by examples taken from our work but restricted to materials in which at least one component is a metal oxide. We will exclusively discuss CVD and sol–gel methods, however, for the sake of completeness it should be stated (even considering results obtained from similar or other techniques) that the key point in the syntheses of the materials is not the technique but the correct choice of the precursor and its inherent chemical reactivity.

Control of stoichiometry in the precursor and material ($BaTiO_3$ and related pervoskites, SSP-I)

To demonstrate the advantages of the single source precursor method (containing the metallic elements in a correct stoichiometry in a single molecule, SSP-I) over classical multi-source procedures in a sol–gel synthesis of oxide powders, we have made a systematic study with barium titanate and related pervoskites.[31] In this study we first evaluate classical procedures like a sol–gel hydroxide route using an equimolar mixture of $Ba(OH)_2{\cdot}8H_2O$ and $Ti(O^iPr)_4$ in iso-propanol/acetic anhydride and an acetate sol–gel route using again iso-propanol/acetic anhydride to which $Ti(O^iPr)_4$ and barium acetate is added. The oxide powders obtained from these two synthetic approaches are compared to powders obtained using a mixed metal alkoxide-hydroxide $[BaM(OH)(O^iPr)_5(HO^iPr)_3]_2$ (M = Ti, Zr) as the SSP.

At this stage it is interesting to note, that the mixed metal alkoxides described before are not available in a straight forward manner.[32] For example, if $[Ba(O^tBu)_2]_n$ is reacted with $M(O^tBu)_4$ (M = Ti, Zr) in a 1 : 1 or 1 : 2 ratio in non-coordinating solvents, the compound $BaM_2(O^tBu)_{10}$ is formed [see eqn. (4)].

$$1/n[Ba(O^tBu)_2]_n + 2M(O^tBu)_4 \longrightarrow \underset{M = Ti, Zr}{BaM_2(O^tBu)_{10}} \quad (4)$$

The molecular structure of the Ba–Zr alkoxide (Zr : Ba = 2 : 1) is depicted in Fig. 1. If the *tert*-butyl group attached at the oxygen is replaced by an iso-propyl group (for M = Ti), either the corresponding $[BaTi_2(O^iPr)_{10}]_2$ compound is formed (which is dimeric and with different coordination spheres in contrast to the *tert*-butyl derivative) or the compounds $Ba[Ti_2(O^iPr)_9]_2$ and $[Ti(O^iPr)_5]Ba[Ti_2(O^iPr)_9]$ [see also eqn. (5)].[33]

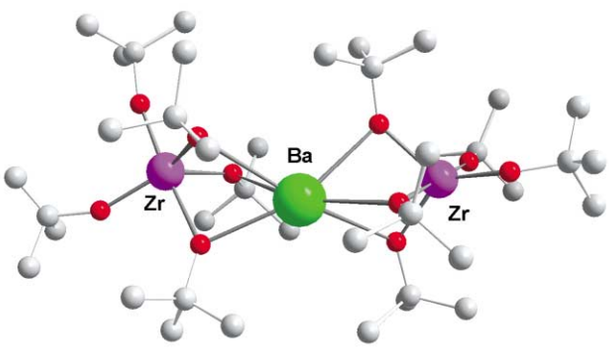

Fig. 1 Molecular structure of $BaZr_2(O^tBu)_{10}$ from a single-crystal X-ray determination.[32] As in the other figures all oxygen atoms are red and all carbon atoms are grey. As in Figs. 2 and 3, hydrogen atoms have been omitted for clarity.

$$3/n[Ba(O^iPr)_2]_n + xTi(O^iPr)_4 \longrightarrow 1/2[BaTi_2(O^iPr)_{10}]_2 + [Ti_2(O^iPr)_9]Ba[Ti(O^iPr)_5] + Ba[Ti_2(O^iPr)_9]_2 \quad (5)$$

The different products in eqn. (5) can be suppressed in favor of one formula by use of different stoichiometries or by adding iso-propanol (see ref. 33). It becomes clear from these results that mixed barium/titanium–iso-propanolates with stoichiometry Ba : Ti = 1 : 1 are not obtainable by the chosen route. The titanium and zirconium atoms are Lewis acidic and form simple negatively charged entities of the type $[M(OR)_5]^-$ or $[M_2(OR)_9]^-$. The structure of the Ba–Ti alkoxide combining both of these anions is depicted in Fig. 2. The use of *tert*-butoxy instead of iso-propoxy as ligand favors the monometallic anion and thus shifts the stoichiometry in the mixed

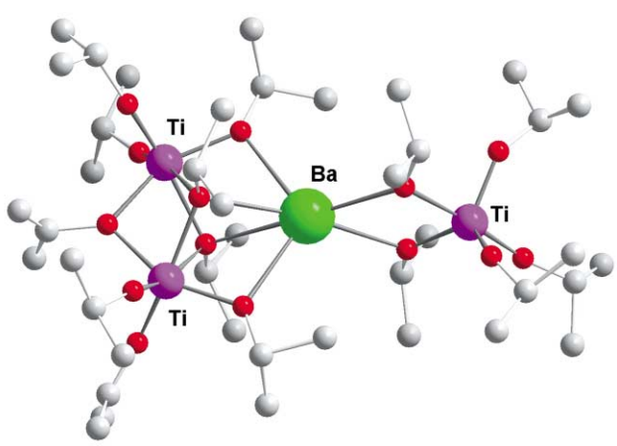

Fig. 2 Molecular structure of $BaTi_3(O^iPr)_{14}$ ($[Ti(O^iPr)_5]Ba[Ti_2(O^iPr)_9]$) from XRD.[33]

alkoxide to the desired ratio although the ideal value is not obtained.

We have tried to overcome the difficulties described so far by using bases such as tetrahydrofuran in order to coordinate the barium center and thus alter its reaction with $Ti(O^tBu)_4$ or $Zr(O^tBu)_4$. Surprisingly, when *tert*-butanol is not completely eliminated a crystalline compound with a metal ratio, Ba : Zr, of 2 : 1 $[Ba_2Zr(O^tBu)_8(HO^tBu)\cdot 2THF]$ is formed.[32] The result of the structural analysis of this compound is depicted in Fig. 3. If the same reaction is performed with the strict exclusion of

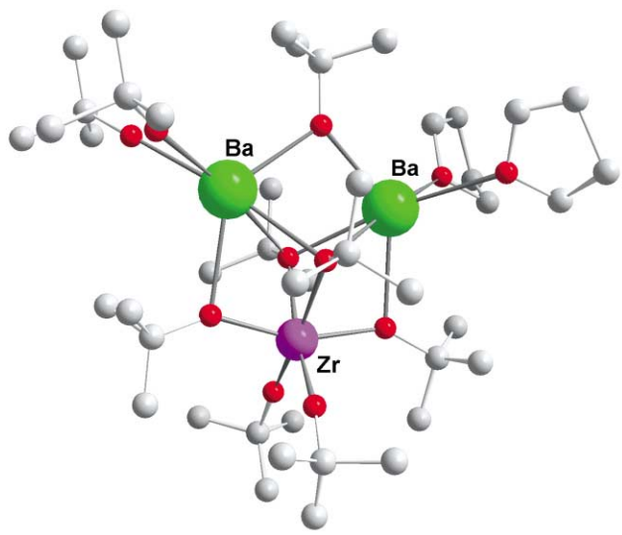

Fig. 3 Molecular structure of $Ba_2Zr(O^tBu)_8(HO^tBu)\cdot 2THF$ from XRD.[32] There is a O–H–O bridge on the terminal *tert*-butoxy groups of one of the barium atoms.

tert-butanol, the molecule $BaZr(O^tBu)_6\cdot 2THF$ forms at low temperatures as a metastable crystalline compound. It has the desired metal atom ratio of 1 : 1, but is difficult to handle. Fortunately, it can be transformed to a THF free, crystalline and stable aggregate, $[BaZr(OH)(O^iPr)_5(HO^iPr)_3]_2$, in good yields by ligand exchange and partial hydrolysis in iso-propanol; the whole reaction sequence is shown in eqn. (6).[32]

$$1/n[Ba(O^tBu)_2]_n + Zr(O^tBu)_4 + 2THF \longrightarrow 1/m[BaZr(O^tBu)_6\cdot 2THF]_m$$
$$1/m[BaZr(O^tBu)_6\cdot 2THF]_m + H_2O + 8\,{}^iPrOH \longrightarrow 6\,{}^tBuOH + 2THF + 1/2[BaZr(OH)(O^iPr)_5(HO^iPr)_3]_2 \quad (6)$$

The $Ba_2Zr_2O_6$ core of the molecule is centrosymmetric and may be described as two *seco*-norcubane units fused along a common Ba_2O_2 face (compare also Fig. 4). The analogous titanium derivative $[BaTi(OH)(O^iPr)_5(HO^iPr)_3]_2$ as well as the Zr–Ti mixed $[Ba_2TiZr(O^iPr)_{12}]$ have also been obtained.[31]

The single source precursor route using $[BaM(OH)(O^iPr)_5(HO^iPr)_3]_2$ M = Ti, Zr and $[BaTi_{0.5}Zr_{0.5}(O^iPr)_6]_2$ in 3.0 M aqueous solution in iso-propanol was compared to the hydroxide route and to the acetic anhydride route.[31] The oxide powders $BaTiO_3$ (BT), $BaZrO_3$ (BZ) und $BaTi_{0.5}Zr_{0.5}O_3$ (BZT) obtained from these three different procedures were characterized using X-ray powder diffraction, scanning electron microscopy (SEM) combined with energy dispersive X-ray (EDX), transmission electron microscopy and classical elemental analysis. The heat treatment of the intermediate gels and the sintering of the powders was followed by DTA/TGA measurements. The following conclusions can be drawn:

The molecular level mixing and the strict equimolarity of the metallic elements as well as the preformed oxygen–metal framework of the mixed metal alkoxide precursors allow high compositional purity, low crystallization temperatures and nano-dimensions with low dispersity. In Fig. 5 a sequence of

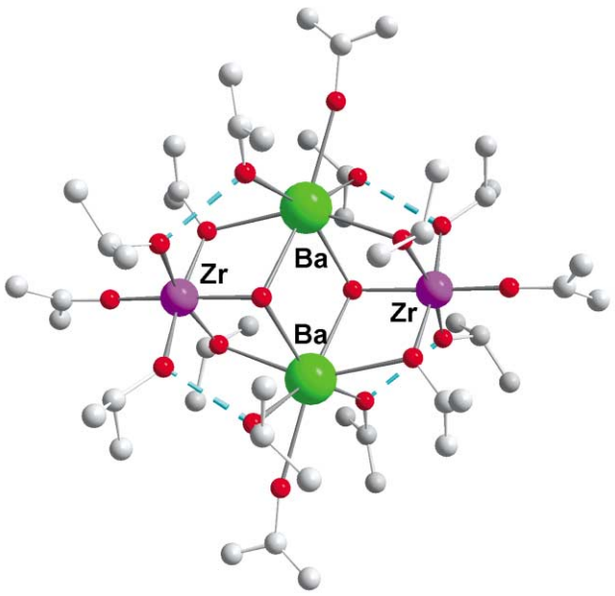

Fig. 4 Molecular structure of $[BaZr(OH)(O^iPr)_5(HO^iPr)_3]_2$ from XRD.[32] The hydrogen atoms of the hydroxide, the alcohol ligands and of the alkyl groups are not drawn (see also Figs. 1–3). The hydrogen bonds between alcohol and alcoholate ligands are represented by dotted lines.

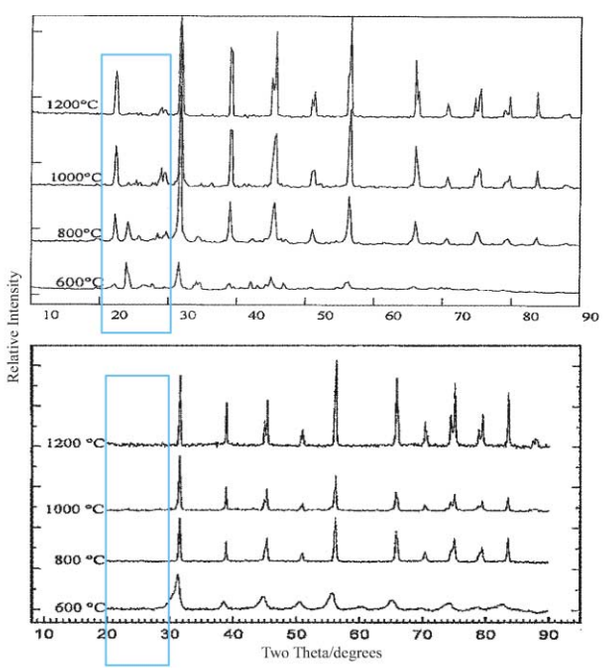

Fig. 5 X-Ray powder diffraction diagrams at different temperatures for heat treated $BaTiO_3$ gels from the single source precursor alkoxide route (top) and the acetate route (bottom). Some easily distinguishable lines of undesired phases are highlighted by the blue frames.

X-ray powder diffraction diagrams obtained at different temperatures from the SSP-I route and from the acetate route are compared (the results from the hydroxide route are similar to the acetate process). From these diagrams it is obvious that even at 1200 °C $BaTiO_3$ obtained using the sol–gel acetate route is still contaminated by impurities such as $BaCO_3$ and Ba_2TiO_4 while $BaTiO_3$ obtained from the sol–gel single precursor is formed in a pure state at 600 °C! The broad reflections in the diagram of the SSP product reflect the nanocrystallinity of the samples which can be transformed to larger crystallites on heating. The crystal diameters of the powders obtained by the acetate route range from 30–100 nm at 600 °C and grow less evenly with temperature than in the SSP route. In Fig. 6 the particle size distribution functions [determined by two different

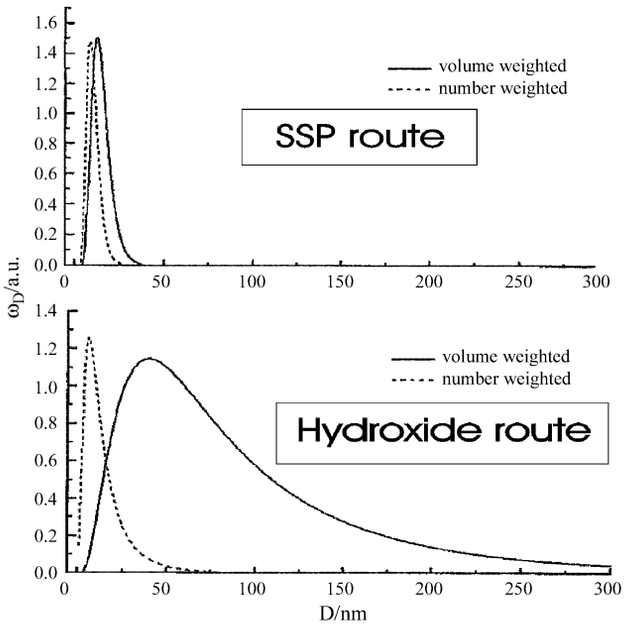

Fig. 6 Particle size distribution curves of $BaZrO_3$ powders obtained at 600 °C *via* the alkoxide (SSP route) and hydroxide route.[31]

methods from X-ray diffraction[31] for $BaZrO_3$ prepared *via* alkoxide (SSP) and hydroxide routes] reveal that despite the different mean sizes the functions for the alkoxide process are narrower. This may lead to important applications, especially if small variations of crystallite sizes are needed.

Cascade reactions to form high purity materials: $MgAl_2O_4$ from an alkoxy-hydride (SSP-II)

Spinels of the composition MM'_2O_4 (M = two valent metal atom, M′ = three valent metal atom) synthesized by sol–gel or similar processes can be obtained as nano-meter sized crystallites and are of broad and general interest because of their applications.[34–39] In our laboratory single source precursors of the type $M[Al(OR)_4]_2$ (M = Mg, Fe, Co, Ni, Cu, Zn; R = ^{i}Pr, ^{t}Bu) have been used in water/oil microemulsion sol–gel techniques[40,41] or in simple iso-propanol/water mediated sol–gel routes to obtain nanoscaled spinel powders.[42] The spinel $MgAl_2O_4$ has also been prepared by classical techniques.[43,44]

As an example of the single source precursor strategy II (SSP-II) we describe here the synthesis, the molecular structure and the stepwise degradation of $[MgAl_2(O^tBu)_4H_4]$, a "mixed metal mixed ligand precursor".[45] The molecule is synthesized in two steps as can be seen from eqn. (7).

$$4LiAlH_4 + 8\,{}^tBuOH \longrightarrow [Li(O^tBu)_2AlH_2]_4 + 8H_2$$
$$[Li(O^tBu)_2AlH_2]_4 + 2MgCl_2 \longrightarrow 2Mg[(O^tBu)_2AlH_2]_2 + 4LiCl \quad (7)$$

A compound equivalent to the magnesium–aluminium alkoxohydride can be obtained from $LiAlD_4$, with the sole difference that all hydridic atoms are substituted by deuterium atoms. The molecular structure of the hydride derivative, as found from X-ray diffraction techniques, is shown in Fig. 7. Whereas the magnesium atom is exclusively bonded to oxygen atoms, each aluminium atom has oxygen as well as hydride ligands in a tetrahedral coordination sphere. The molecule $Mg[(O^tBu)_2AlH_2]_2$ is very volatile (sublimation point: 40 °C at 10^{-3} atm) and can be handled under an inert gas atmosphere with strict exclusion of oxygen and water. In a CVD apparatus, in which an inductively heated metal target is brought into the gas flow (which consists only of the precursor and argon), a

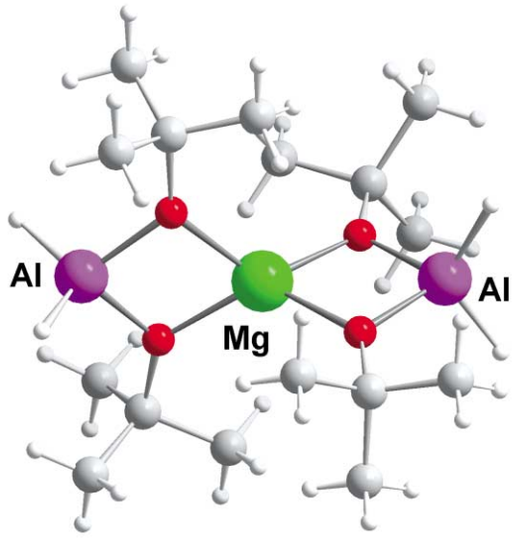

Fig. 7 Molecular structure of $Mg[(^tBuO)_2AlH_2]_2$ from XRD with all atoms shown.[45]

quadrupole mass spectrometer is directly linked to the CVD reactor to register all volatiles in an on-line fashion.[46]

When the temperature is steadily raised to 350 °C, the mass spectrum changes dramatically indicating the simultaneous evolution of hydrogen and iso-butylene. Taking $Mg[(O^tBu)_2AlD_2]_2$ in place of the hydrido alkoxide shows a drastic reduction in the intensity of the peak at m/z = 2 (H_2) and the appearance of a new peak at m/z = 3 (HD). In Fig. 8, a typical mass spectrum is

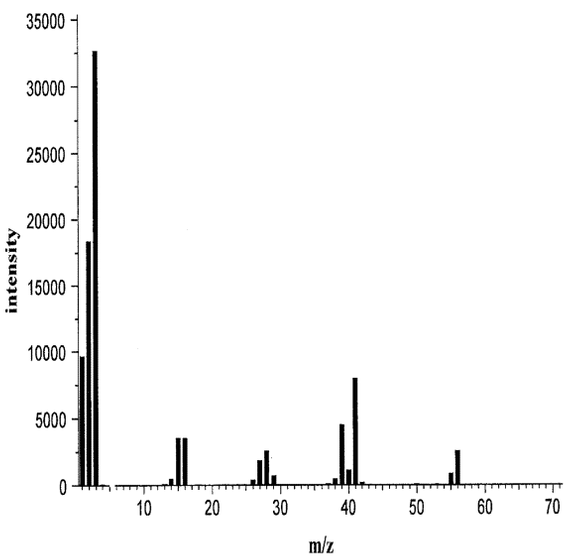

Fig. 8 Mass spectrum of the degradation of $Mg[(^tBuO)_2AlD_2]_2$ showing signals due to iso-butylene (including masses at m/z = 1 and 2) and HD (m/z = 3).

depicted which shows besides the signals of iso-butylene those of HD (m/z = 3). In an independent experiment the decomposition gases, except hydrogen, were trapped (at −196 °C), and identified by ^{1}H- and ^{13}C-NMR spectroscopy as iso-butylene. The findings seem to indicate that two reactions occur, presumably in a cascade fashion: a) the negatively charged hydride (deuteride) combines with one of the positively charged hydrogen atoms of the *tert*-butyl groups; b) the remaining charge on the methylene carbon atoms redistributes with elimination of iso-butylene. The corresponding mechanism of these combined reactions is depicted in Scheme 1.

$Mg[(O^tBu)_2AlH_2]_2$ and its deuterated derivative thus contain ligands which mutually interact on thermal induction, liberating two volatile gases and forming the planned combination of

$$Mg\{[(H_3C)_3C\text{-}O]_2AlD_2\}_2 \longrightarrow 4\ HD + 4\ H_2C{=}C(CH_3)_2 + MgAl_2O_4$$

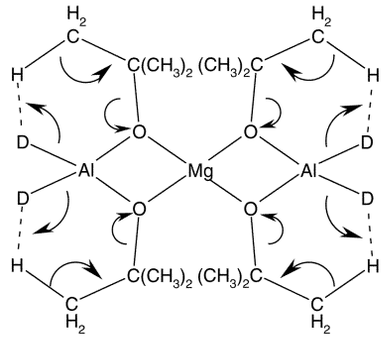

Scheme 1 Thermally induced degradation of $Mg[(O^tBu)_2AlD_2]_2$ to $MgAl_2O_4$.

elements, $MgAl_2O_4$, on a molecular scale. It is not astonishing that the obtained oxide powder (oxide coating) is chemically pure (content of C less than 0.4%), nano-scaled (at 450 °C/0.5 h average particle diameters are less than 10 nm), and perfectly colorless. Samples obtained at 450 °C are already crystalline (X-ray powder diffraction diagram). Small angle X-ray scattering (SAXS) reveals the primary diameters of the $MgAl_2O_4$ particles obtained at 450 °C to be in the range of 7.2 nm, in good agreement with the line width fitting of the powder X-ray diffraction diagrams, and to be partially agglomerated to larger particles with a mean diameter of 110 nm.[47] The particles at 450 °C thus seem to begin to form a fractal system. At higher target temperatures (600 °C) these fractal systems seem to disappear and only mono-modal particles are found, which are somewhat larger (mean diameter = 11.2 nm). As a conclusion of this example of the SSP-II method it can be noted that besides the high purity of the $MgAl_2O_4$ ceramic, nano-crystalline particles are obtained at temperatures of 400–600 °C, lower than by alternative sol–gel or CVD techniques, and that the transformation of the precursor to the ceramic is almost quantitative.

Multiphasic solid state systems (metal/metal oxide, alloy/metal oxide, metal oxide/metal oxide) from single source precursors (SSP-III)

In this section we will deal with procedures in which a mixture of solid phases is obtained (the general reaction, eqn. (3), has been designated as SSP-III from a single molecule). We first discovered one of these procedures in 1994,[46] when we thermolyzed (350 °C) the volatile $BaSn_2(O^tBu)_8$ in a CVD process. The reaction is summarized in eqn. (8).

$$BaSn_2[OC(CH_3)_3]_6 \longrightarrow 3\,^tBu\text{–}OH\uparrow + 3H_2C{=}C(CH_3)_2\uparrow + Sn + BaSnO_3 \quad (8)$$

The key step of this reaction is the disproportionation of two valent tin in the starting molecule into tin(IV) and tin(0) with the loss of iso-butylene and *tert*-butanol. As shown in reaction (8) formation of each tin(0) atom results in the concomitant formation of the corresponding tin(IV) species, the tin(0)/tin(IV) ratio being strictly 1.0. The 1 : 1 correspondence of *tert*-butanol and iso-butylene can be deduced from the mass spectral and NMR analysis of the trapped gases. Apparently, the proton left behind after elimination of iso-butylene recombines with the *tert*-butanolate to form *tert*-butanol.

The disproportionation reaction shown for $BaSn_2(O^tBu)_6$ can be transposed to other elements of Group 14, and can be modified by using other precursor molecules.[48] In Table 1 a compilation of biphasic systems synthesized by this procedure is given.

As may be anticipated from the molecular approach, the metallic element and the metal oxide are liberated on an atomic level at the same time and could quickly associate within short

Table 1 Molecular precursors and composites obtained from CVD[48]

Precursor	Composite
$[Ge(O^tBu)_2]_2$	α-Ge/GeO_2
$[Sn(O^tBu)_2]_2$	β-Sn/SnO_2
$[Pb(O^tBu)_2]_3$	Pb/PbO_2
$SrGe_2(O^tBu)_6$	α-Ge/$SrGeO_3$
$BaGe_2(O^tBu)_6$	α-Ge/$BaGeO_3$
$CaSn_2(O^tBu)_6$	β-Sn/$CaSnO_3$
$SrSn_2(O^tBu)_6$	β-Sn/$SrSnO_3$
$BaSn_2(O^tBu)_6$	β-Sn/$BaSnO_3$
$CaPb_2(O^tBu)_6$	Pb/$CaPbO_3$
$BaPb_2(O^tBu)_6$	Pb/$BaPbO_3$

time intervals, *i.e.* before phase separation starts. Interestingly, the biphasic systems of Table 1 all form fractals, as can be deduced by closer inspection of the composites. One of these fractals, which can be described as globular assemblies of ball-shaped species, is shown in Fig. 9. The smallest entities we were

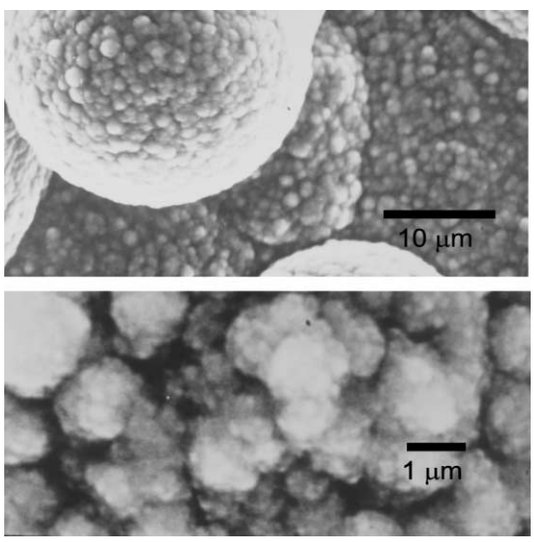

Fig. 9 SEM pictures of the composite Sn/$BaSnO_3$ (same specimen but with different scaling) with fractal assemblies of ball-shaped entities.

able to analyze have a metallic core wrapped up by the metal oxide (XPS, XRD and EDX evidence).[48] The dimensions of the metallic core and the metal oxide shell may vary with the precursor system, temperature, pressure and time of exposure, but could be smaller than 1–5 nm.

A crucial condition for these biphasic systems to maintain their fractal nature is the use of a dynamic vacuum (pumping off all volatile gases like *tert*-butanol and iso-butylene). In a model reaction [using tin(II) *tert*-butoxide as precursor] we have compared the results obtained in a dynamic vacuum with those obtained from a static system under 1 atm N_2 pressure and identical temperatures.[49] In contrast to the Sn/SnO_2 composite formed in a dynamic vacuum, the sole solid compound in the static system was SnO (romachite, XRD evidence). The liberated gases were identical in the two processes. Using temperatures 300–400 °C higher than in the dynamic vacuum process also gave Sn/SnO_2 composites in the static process, but with no noticeable fractality. Instead the two phases were well separated forming tin and tin dioxide particles of μm dimensions.

An even more complex composite of an intermetallic and oxide phase has been obtained by CVD of the volatile bimetallic alkoxide $Ni_2Sn_2(O^tBu)_8$.[50] The solid product is a mixture of the alloy Ni_3Sn_4 and tin dioxide. In Fig. 10 a high resolution transmission electron micrograph is shown, illustrating the two mixed-up phases. The whole process of thermolysis is quite complex and is due to partial decomposition of the precursor as shown in eqn. (9).

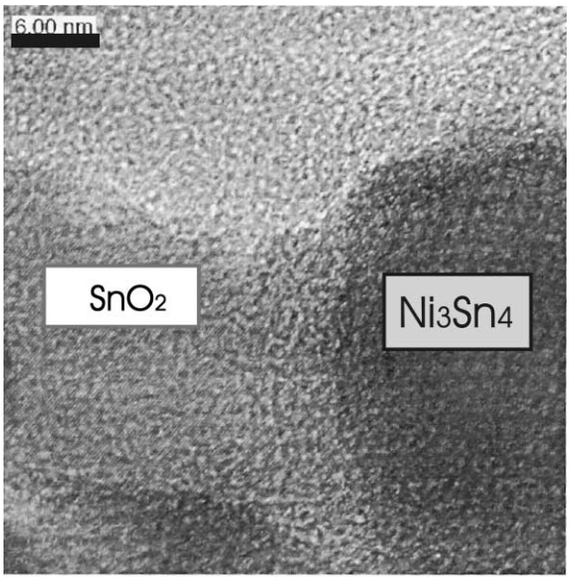

Fig. 10 HR-TEM image of the composite Ni_3Sn_4/SnO_2.

$$1/2[Ni_2Sn_2(O^tBu)_8] \rightleftharpoons 1/2[Sn(O^tBu)_2]_2 + 2/n[Ni(O^tBu)_2]_n \quad (9)$$

Whereas $[Sn(O^tBu)_2]_2$ under the experimental conditions disproportionates and decomposes in the usual way to Sn and SnO_2 (see above), the nickel alkoxide part liberates *tert*-butanol and iso-butylene as well and transforms to NiO. Below 500 °C a deposition of a solid is observed which contains the phases NiO, Sn and SnO_2 (as deduced from XPS and XRD). When the temperature of the whole CVD process is raised to 550 °C a redox reaction seems to occur and the phases formed are Ni_3Sn_4 and tin dioxide [eqn. (10)].

$$3NiO + 5.5Sn + SnO_2 \longrightarrow Ni_3Sn_4 + 2.5SnO_2 \quad (10)$$

The solid phases have been identified by XPS, Mössbauer spectroscopy, HRTEM, XRD and the ratios have been determined in a typical sample as 14 mol% Ni_3Sn_4 and 86 mol% SnO_2 (Sn : Ni = 3.38; Sn(IV) : Sn(0) = 1.54). The lower Ni content in the solid compared to the precursor is due to the equilibrium of eqn. (9), as $[Ni(O^tBu)_2]_n$ is less volatile than the other components $[Sn(O^tBu)_2]_2$ or $[Ni_2Sn_2(O^tBu)_8]$.

To demonstrate the potential of the SSP-III procedure in the formation of biphasic materials we have used two lanthanide aluminates $[LnAl(O^iPr)_6(HO^iPr)]_2$ and $[LnAl_3(O^iPr)_{12}(HO^iPr)]$ (Ln = Nd, Pr) in CVD[51] and sol–gel[52] processes and the results obtained have been compared to materials produced by classical glycol and solid state syntheses.[53] The results of single crystal structure determinations on the neodymium derivatives are presented in Fig. 11. Apparently, the Nd : Al ratio is different in the two molecules which has a crucial consequence for the CVD or sol–gel procedure. In eqns. (11) and (12) the two reactions

$$[NdAl(O^iPr)_6(HO^iPr)]_2 \xrightarrow[\{-{}^i\text{PrOH}\}]{1)\ {}^i\text{PrOH}/H_2O,\ 2)\ \Delta T} NdAlO_3 \quad (11)$$

$$[NdAl_3(O^iPr)_{12}(HO^iPr)] \xrightarrow[\{-{}^i\text{PrOH}\}]{1)\ {}^i\text{PrOH}/H_2O,\ 2)\ \Delta T} NdAlO_3/Al_2O_3 \quad (12)$$

occurring for the sol–gel process are given (in CVD made with $[NdAl_3(O^iPr)_{12}(HO^iPr)]$ the volatile gases are ^{i}PrOH, CH_2=CH–CH_3, acetone and hydrogen, the solid compound being almost identical with the sol–gel route).[51]

The solid phases obtained from eqns. (8) and (9) have been characterized using elemental analyses, TG/DTA (firing step), X-ray powder diffraction, electron microscopic methods (SEM,

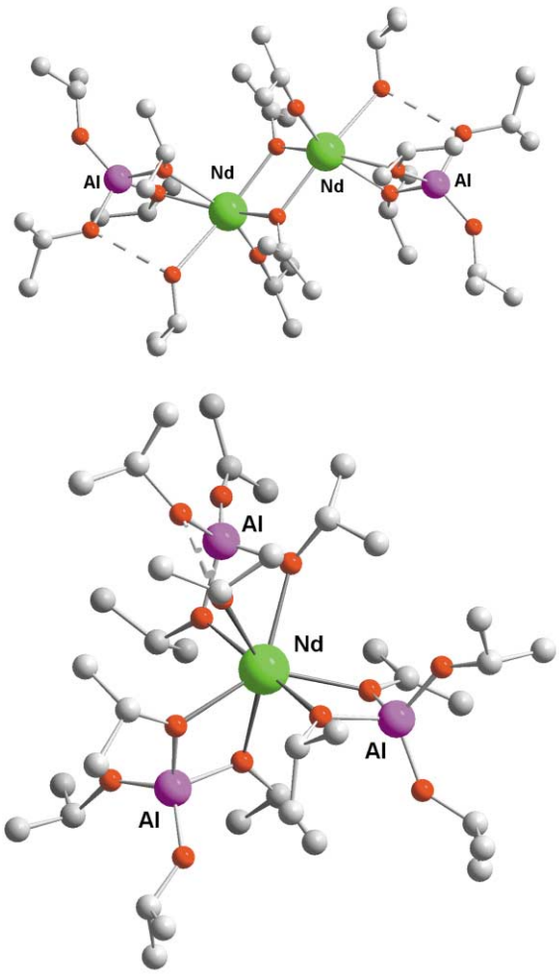

Fig. 11 Results of X-ray structure determinations on $[NdAl(O^iPr)_6(HO^iPr)]_2$ and $[NdAl_3(O^iPr)_{12}(HO^iPr)]$. The dotted lines show the hydrogen bridges, the hydrogen atoms have been omitted for clarity.

TEM, HR-TEM), ^{27}Al-NMR, XPS and optical absorption spectra. The following facts can be deduced:

a) The molar ratio of the metallic elements in the precursor is strictly maintained in the solid products. Thus, the misfit of Nd : Al ratio in $[NdAl_3(O^iPr)_{12}(HO^iPr)]$ with respect to $NdAlO_3$ results in the parallel formation of Al_2O_3! The two phases $NdAlO_3$ and Al_2O_3 are formed in an exact 1 : 1 ratio as can be seen from the XPS spectrum of the composite (Fig. 12). As the

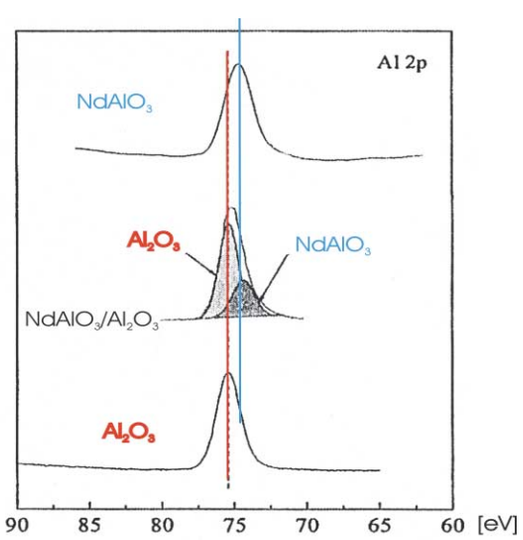

Fig. 12 XPS-spectrum of the composite $NdAlO_3/Al_2O_3$ with deconvolution and comparison to the single phases $NdAlO_3$ (top) and Al_2O_3 (bottom).

temperature of the elimination of volatiles from the gel is maintained below 800 °C no other compounds or phases form. When $[NdAl(O^iPr)_6(HO^iPr)]_2$ is used the product of the sol–gel or CVD process is pure $NdAlO_3$. Again the SSP concept and the moderate temperatures give nano-scaled species in both cases.

b) The $NdAlO_3$ phase in the metal oxide composite is crystalline while Al_2O_3 remains amorphous up to 1200 °C. The different tendency of crystallization between the two phases may be linked to the higher heat capacity of $NdAlO_3$ compared to Al_2O_3. On the same line, despite the ultra homogeneous mixing of the two phases in the early stages of the sol–gel process the TEM images clearly indicate a microstructure which may be described as well separated $NdAlO_3$ nano crystals of 70 nm diameter (1000 °C) equally distributed in the Al_2O_3 matrix. This microstructure is typical for the alkoxide SSP-III route and completely different from the glycolate product which has been obtained in a parallel control synthesis in which the $NdAlO_3$ crystallites agglomerate and form grains of clustering nano particles of different sizes.

c) The physical consequences of the biphasic composite obtained *via* the SSP-III route are multiple,[53] the optical ones being the most intriguing. We have found that the composite material shows a 35 times enhancement in the photoluminescence intensity of the rare earth cation compared to the single phase $NdAlO_3$, which shows the usually observed quenching! The interface $NdAlO_3$–Al_2O_3 in the composite system may be responsible for this effect which maintains the Nd–Nd separation on the surface and between the crystalline grains at an ideal value. This new aspect of phase separation can, in a certain way, also be transposed to classical optical materials such as neodymium doped $Y_3Al_5O_{12}$.[54]

Conclusion

Chemistry plays an important part in the development of new materials, both from a conceptual point of view and *via* the tuning of microstructures. There is no doubt that the single source precursor processes discussed in this article are, from a first impression, more laborious and expensive than a classical process using cheap materials and simple chemicals. On the other side, once a single source precursor has been designed, its upscaling could reduce the expenses, and the more tedious work at the beginning of the syntheses could be compensated by materials with better properties (no cleaning process necessary, simple control of the process parameters, high efficiency and yield *etc*.) In my opinion, processes other than CVD or sol–gel may be used in a similar way in the syntheses of materials, but in all of these the chemical input is of upmost importance.

Acknowledgements

I would particularly like to thank all the people who have contributed to the results presented above: S. Mathur, whom I thank for enthusiastic help and fruitful discussions, V. Huch for assistance with the X-ray structure determinations, S. Kneip and S. Faber for their discoveries, M. Zimmer for the solid state NMR work as well as many excellent chemists and physicists like A. Altherr, N. Lecerf, H. Shen and E. Fritscher. My colleagues S. Hüfner, R. Hempelmann and H. P. Beck have assisted our work through fruitful collaborations. Finally, we would like to thank the Fonds der Chemischen Industrie, the DFG (SFB-Program: SFB 277) and the Saarland University for their financial support.

References

1 Some examples: *J. Mater. Chem.*, *Chem. Vap. Deposition*, *Nanostruct. Mater.*, *J. Mater. Res.*, *Chem. Mater.*, *Adv. Mater.*, *J. Sol–Gel Sci. Technol.*, *etc*.

2 H. O. Pierson, *Handbook of Chemical Vapour Deposition*, Noyes Publications, Park Ridge, USA, 1992.
3 T. T. Kodas and M. J. Hamden-Smith, *The Chemistry of Metal CVD*, VCH, Weinheim, Germany, 1994.
4 W. S. Rees Jr., *CVD of Non Metals*, VCH, Weinheim, Germany, 1996.
5 C. J. Brinker and G. W. Scherer, *Sol–Gel-Science: The Physics and Chemistry of Sol–Gel Processing*, Academic Press, Boston, USA, 1990.
6 C. Sanchez and F. Ribot, *New J. Chem.*, 1994, **18**, 1007.
7 H. K. Schmidt, *J. Sol–Gel Sci. Technol.*, 1997, **8**, 557.
8 H. K. Schmidt, *Chem. Unserer Zeit*, 2001, **35**, 176.
9 L. L. Hench and J. K. West, *Chem. Rev.*, 1990, **90**, 33.
10 M. A. Hermann and H. Sitter, *Molecular Beam Epitaxy*, Springer, Berlin, Germany, 1989.
11 N. Hüsing and U. Schubert, *Angew. Chem.*, 1998, **110**, 22; N. Hüsing and U. Schubert, *Angew. Chem., Int. Ed.*, 1998, **37**, 22.
12 W. Mörke, R. Lamber, U. Schubert and B. Breitscheidel, *Chem. Mater.*, 1994, **6**, 1659.
13 R. J. P. Corriu, *Angew. Chem.*, 2000, **112**, 1433; R. J. P. Corriu, *Angew. Chem., Int. Ed.*, 2000, **39**, 1377.
14 G. Philipp and H. Schmidt, *J. Non-Cryst. Solids*, 1984, **63**, 283.
15 G. Jangg, in *New Materials by Mechanical Alloying Techniques*, eds. E. Arzt and L. Schulz, DGM (Deutsche Gesellschaft für Materialkunde), Frankfurt, Germany, 1998, p. 39.
16 P. Balaz, *Extractive Metallurgy of Activated Minerals (Process Metallurgy 10)*, Elsevier, Amsterdam, 2000.
17 C. R. Clayton, J. K. Hirvonem and A. R. Srivatsa, eds., *Advances in Coatings Technologies for Surface Engineering*, Minerals, Metals & Materials Soc. (TMS), Warrendale, Pennsylvania, USA, 1997.
18 H. Gleiter, *Acta Mater.*, 2000, **48**, 1.
19 J. H. Fendler, ed., *Nanoparticles and Nanostructured Films*, Wiley-VCH, Weinheim, Germany, 1998.
20 A. S. Edelstein, J. S. Murday and B. B. Rath, *Prog. Mater. Sci.*, 1997, **42**, 5.
21 (*a*) D. C. Bradley, *Chem. Rev.*, 1989, **89**, 1317; (*b*) R. C. Mehrotra, *Chemtracts: Inorg. Chem.*, 1990, **2**, 338.
22 (*a*) S. Hirano, T. Hayashi, K. Noaski and K. Kato, *J. Am. Ceram. Soc.*, 1989, **72**, 707; (*b*) D. J. Eichrost, D. A. Payne, S. R. Wilson and K. E. Howard, *Inorg. Chem.*, 1990, **29**, 1458.
23 R. Narayanau and R. M. Laine, *Appl. Organomet. Chem.*, 1997, **11**, 919.
24 W. A. Herrmann, N. W. Huber and O. Runte, *Angew. Chem.*, 1995, **107**, 2371; W. A. Herrmann, N. W. Huber and O. Runte, *Angew. Chem., Int. Ed. Engl.*, 1995, **34**, 2187.
25 L. G. Hubert-Pfalzgraf, *New J. Chem.*, 1987, **11**, 663.
26 M. Veith, S. Mathur and C. Mathur, *Polyhedron*, 1998, **17**, 1005.
27 M. Veith, S. Kneip, S. Faber and E. Fritscher, *Mater. Sci. Forum*, 1998, **269–272**, 303.
28 M. Veith, A. Rammo, S. Faber and B. Schillo, *Pure Appl. Chem.*, 1999, **71**, 401.
29 M. Veith, *Mater. Sci. Forum*, 2000, **343–346**, 531.
30 M. Veith, S. Mathur and V. Huch, *J. Am. Chem. Soc.*, 1996, **118**, 903.
31 M. Veith, S. Mathur, N. Lecerf, V. Huch, T. Decker, H. P. Beck, W. Eiser and R. Haberkorn, *J. Sol–Gel Sci. Technol.*, 2000, **15**, 145.
32 M. Veith, S. Mathur, V. Huch and T. Decker, *Eur. J. Inorg. Chem.*, 1998, 1327.
33 M. Veith, S. Mathur and V. Huch, *Inorg. Chem.*, 1997, **36**, 2391.
34 A. Edelstein and R. C. Cammerata, eds., *Nanomaterials: Synthesis, Properties and Applications*, Institute of Physics Publishing, Bristol, UK, and Philadelphia, USA, 1996.
35 K. E. Sickfaus and J. M. Wills, *J. Am. Ceram. Soc.*, 1998, **82**, 3279.
36 P. P. Phule and S. H. Risbud, *J. Mater. Sci.*, 1990, **25**, 1169.
37 A. K. Adak, S. K. Saha and P. Pramanik, *J. Mater. Sci. Lett.*, 1997, **16**, 234.
38 J. E. Baker, R. Burch and N. Yugin, *Appl. Catal.*, 1991, **73**, 135.
39 S. Rezgui and B. C. Gates, *J. Non-Cryst. Solids*, 1997, **210**, 287.
40 F. Meyer, R. Hempelmann, S. Mathur and M. Veith, *J. Mater. Chem.*, 1999, **9**, 1755.
41 F. Meyer, A. Dierstein, Ch. Beck, W. Härtl, R. Hempelmann, S. Mathur and M. Veith, *Nanostruct. Mater.*, 1999, **12**, 71.
42 S. Mathur, M. Veith, M. Haas, H. Shen, N. Lecerf, V. Huch, S. Hüfner, R. Haberkorn, H. P. Beck and M. Jilavi, *J. Am. Ceram. Soc.*, 2001, **84**, 1921.
43 R. E. Rocheleau, Z. Zhang, J. W. Gilje and J. A. Meese-Marktscheffel, *Chem. Mater.*, 1994, **6**, 1615.
44 J. Zhang, G. T. Stauf, R. Gardiner, P. v. Buskirk and J. Steinbeck, *J. Mater. Res.*, 1994, **9**, 1333.
45 M. Veith, A. Altherr and H. Wolfanger, *Chem. Vap. Deposition*, 1999, **5**, 87.
46 M. Veith and S. J. Kneip, *J. Mater. Sci. Lett.*, 1994, **13**, 335.
47 R. Winter, M. Quinten, A. Dierstein, R. Hempelmann, A. Altherr and M. Veith, *J. Appl. Crystallogr.*, 2000, **33**, 507.
48 M. Veith, S. J. Kneip, A. Jungmann and S. Hüfner, *Z. Anorg. Allg. Chem.*, 1997, **623**, 1507.
49 M. Veith, N. Lecerf and M. Gasthauer, *Thermec 2000, J. Mater. Proc. Tech.*, Elsevier, Amsterdam, 2001, compact disc.
50 M. Veith, N. Lecerf, S. Mathur, H. Shen and S. Hüfner, *Chem. Mater.*, 1999, **11**, 3103.
51 M. Veith, S. Mathur, N. Lecerf, K. Bartz, M. Heintz and V. Huch, *Chem. Mater.*, 2000, **12**, 271.
52 M. Veith, S. Mathur, H. Shen, N. Lecerf, S. Hüfner and M. H. Jilavi, *Chem. Mater.*, 2001, **13**, 4041.
53 S. Mathur, M. Veith, H. Shen, S. Hüfner and M. H. Jilavi, *Chem. Mater.*, 2002, **14**, 568.
54 M. Veith, S. Mathur, A. Kareiva, M. Jilavi, M. Zimmer and V. Huch, *Chem. Mater.*, 1999, **9**, 3069.